

Electronic Supplementary Information (ESI)

A Near-infrared Emitting MOF Excited with a Low Energy Wavelength: Controlled Encapsulation of Fluorescein Sensitizer at the Time of Crystals Growth

Guillaume Collet, Antonio Hrvat, Svetlana V. Eliseeva, Céline Besnard, Anton Kovalenko, and Stéphane Petoud*

Table of Contents

| | |
|--|---|
| Experimental Details | 2 |
| Reagents | 2 |
| Synthesis of CD-MOF-161 | 2 |
| PXRD | 2 |
| Photophysical Measurements | 2 |
| Optical microscopy imaging | 2 |
| Bio-mimicking tissue phantom | 3 |
| Optical macroscopy imaging | 3 |
| References | 3 |
| Supplementary Figures and Tables | 4 |

Experimental Details

Reagents

The Di-9AC was synthesized and purified as previously reported.¹ N,N-dimethylacetamide (DMA, 99+%, Aldrich chemistry), ammonium formate (99%, Acros Organics), ytterbium(III) acetate hydrate ($\text{Yb}(\text{OAc})_3$, Aldrich), fluorescein sodium salt (Sigma), TBS (Tris buffered saline, 20x concentrated, Calbiochem), Sodium azide (NaN_3 , Sigma), Gelatin from bovine skin (Type B, Sigma), Bovine hemoglobin (Sigma), Intralipids (20% emulsion, Sigma) were used as received.

Synthesis of CD-MOF-161

The fluorescein-loaded CD-MOF-161 crystals were obtained using a synthetic protocol adapted from a methodology that we have published previously.¹ Briefly, the reaction between ytterbium acetate and Di-9AC was prepared in a 4:1 (metal:ligand) ratio in 3.1 mL of DMA by mixing 68 μmol of $\text{Yb}(\text{OAc})_3 \cdot x\text{H}_2\text{O}$ (23.81 mg) with 17 μmol of Di-9AC (7.56 mg). Additionally, 138 μmol of ammonium formate (8.70 mg), 50 μL of deionized water, and 30 μmol of fluorescein sodium salt (11.29 mg) were added. The mixture was sealed in a Pyrex tube, heated to 60°C for 2 days, and then gradually cooled to room temperature at a rate of 2°C/hour. The resulting orange-coloured block crystals were obtained and washed with DMA to remove unreacted materials.

PXRD

Samples were placed on a silicon single crystal substrate and recovered with Kapton foil. X-ray diffraction patterns were measured using an Empyrean (PANalytical) diffractometer in reflection mode with a monochromated $\text{CuK}\alpha 1$ radiation (Johansson type Ge monochromator) and a PIXcel3D area detector.

Photophysical Measurements

UV-Visible absorption spectra as well as diffuse reflectance spectra were recorded on a Jasco V670 UV-Visible spectrophotometer. Photophysical data were collected on fluorescein-loaded CD-MOF-161 crystals under DMA placed into 2.4 mm i.d. quartz capillaries. Emission and excitation spectra were measured on a custom-designed Horiba Scientific Fluorolog 3 spectrofluorimeter equipped with a visible photomultiplier tube (PMT) (220–850 nm, R928P; Hamamatsu) and a NIR PMT (950–1650 nm, H10330-75; Hamamatsu). Excitation and emission spectra were corrected for the instrumental functions, i.e. variations of the Xenon lamp intensity over the wavelengths range and responses of monochromators and detectors. Luminescence lifetimes were determined under excitation at 355 nm provided by a Nd:YAG laser (YG 980; Quantel). The signals in the NIR were selected using an iHR-320 monochromator (Horiba Scientific) and detected with a Hamamatsu H10330-75 PMT. Output signals from the detector were fed into a 500 MHz bandpass digital oscilloscope (TDS 754C; Tektronix), transferred to a PC for data processing with the program Origin8[®]. Luminescence lifetimes are averages of at least three independent measurements. Quantum yields were determined with the Fluorolog 3 spectrofluorimeter based on an absolute method with the use of an integration sphere (Model G8, GMP SA, Renens, Switzerland). Each sample was measured several times under comparable experimental conditions, varying the positions of samples. Estimated experimental error for the quantum yield determination is 10 %. Detailed information about the experimental procedure are described in the following references: ^{2,3}

Optical microscopy imaging

Epifluorescence microscopy images of MOF crystals were acquired with an inverted Nikon Eclipse Ti microscope equipped with an EMCCD Evolve 512 camera from Photometrics. The Nikon Intensilight C-HGFIE mercury-halide lamp was used as an excitation source. The fluorescein signal was observed using the following set of filters: a 482 nm band pass 35 nm excitation filter, a 506 nm dichroic beam splitter, and a 550 nm band pass 88 nm emission filter. The ytterbium(III) signal was observed using the following set of filters : a 482 nm band pass 35 nm excitation filter, a 801 nm dichroic beam splitter, and a 996 nm band pass 70 nm emission filter. Images were obtained with a Nikon Plan Apo λ 20x and a Nikon Apo TIRF 60x objectives.

Laser confocal scanning microscopy of fluorescein-loaded MOF crystals was performed on an inverted Nikon Eclipse Ti microscope equipped with a Nikon C2si confocal system. The fluorescein dye located inside of the MOF pores was excited with a 488 nm laser while the emitted fluorescence was selectively collected with the spectral detector from 500 to 540 nm. The pinhole was set to obtain optical sections of 0.370 μm thicknesses. Images were obtained with a Nikon Apo TIRF 60x objective.

All microscopy images were collected and processed with Nikon NIS Elements AR and ImageJ softwares.

Bio-mimicking tissue phantom

Bio-mimicking tissue phantoms were prepared according to the research protocol described by Pleijhuis *et. al.*⁴. Briefly, a 15 mL of TBS-azide solution was prepared by adding 15 mg of NaN₃ (15 mM final) to 750 µL of 20x concentrated Tris-buffered saline (TBS, 50 mM Tris and 150 mM NaCl). The presence of azide allows to inhibit the growth of bacteria and to prevent the oxygenation of haemoglobin. The volume was increased to 15 mL by adding deionized water and the pH was adjusted to 7.4. Then, 1.5 g of gelatin was added and the mixture was heated up to 50°C under constant stirring until complete dissolution. Afterward, the mixture was gradually cooled down to 35°C and 165 mg of bovine haemoglobin (final concentration 170 mM) and 750 µL of intralipid 20% emulsion were added to simulate absorption and photon scattering of the tissue, respectively. As a mold to generate layers of 1 mm thickness of bio-mimicking tissue phantom, electrophoresis glass for gels of 1 mm thickness were poured with the mixture at 35°C. After being stored at 4°C for 1 hour, the solidified layers of bio-mimicking tissue phantom was collected after unmounting the electrophoresis glass slides and used.

Optical macroscopy imaging

Epifluorescence macroscopy images of MOF crystals through bio-mimicking tissue were acquired with a Nikon AZ100 microscope equipped with an EMCCD Evolve 512 camera from Photometrics. The Nikon Intensilight C-HGFIE mercury-halide lamp was used as an excitation source. The fluorescein signal was observed using the following filters: a 482 nm band pass 35 nm excitation filter, a 506 nm dichroic beam splitter, and a 550 nm band pass 88 nm emission filter. The ytterbium(III) signal was observed using the following filters : a 482 nm band pass 35 nm excitation filter, a 801 nm dichroic beam splitter, and a 996 nm band pass 70 nm emission filter. Images were obtained with the following macro objectives: Nikon AZ Plan Fluor 5x and Nikon AZ Plan Fluor 2x. For the experiment, a quartz capillary filled with MOF crystals under DMA was covered by a black mask with a 500 µm diameter hole followed by a bio-mimicking phantom tissue of 1 mm thickness. All macroscopy images were collected and processed with Nikon NIS Elements AR and ImageJ softwares.

References

1. G. Collet, T. Lathion, C. Besnard, C. Piguet and S. Petoud, *J. Am. Chem. Soc.*, 2018, **140**, 10820-10828.
2. H. Ishida, J.-C. Bünzli and A. Beeby, *Pure and Applied Chemistry*, 2016, **88**, 701-711.
3. J. C. de Mello, H. F. Wittmann and R. H. Friend, *Advanced Materials*, 1997, **9**, 230-232.
4. R. Pleijhuis, A. Timmermans, J. De Jong, E. De Boer, V. Ntziachristos and G. Van Dam, *J. Vis. Exp.*, 2014, 51776.

Supplementary Figures and Tables

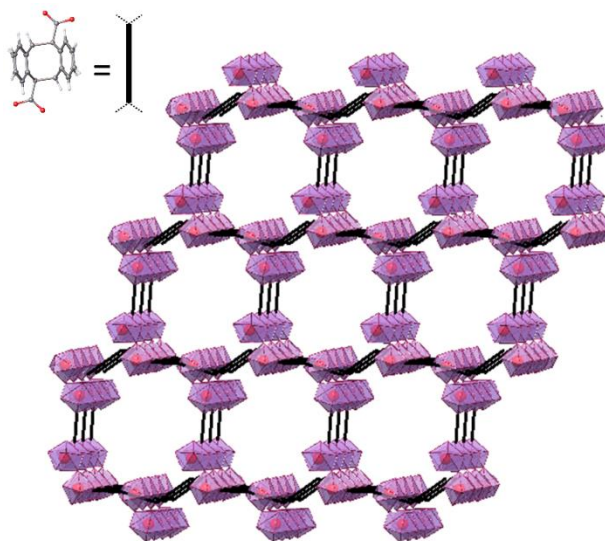


Figure S1: Picture of the crystal structure of the 3D framework of CD-MOF-161. Ligand is represented as black line. Ytterbium metal ions are depicted in red and coordination polyhedron in purple.

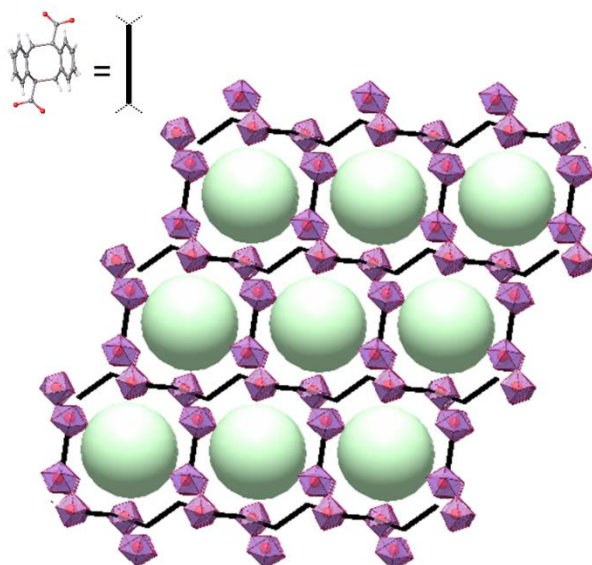


Figure S2: Picture of the crystal structure of FL@CD-MOF-161. Ligand is represented as black line. Ytterbium metal ions are depicted in red and coordination polyhedron in purple. Green spheres represent the fluorescein dyes entrapped inside of MOF pores.

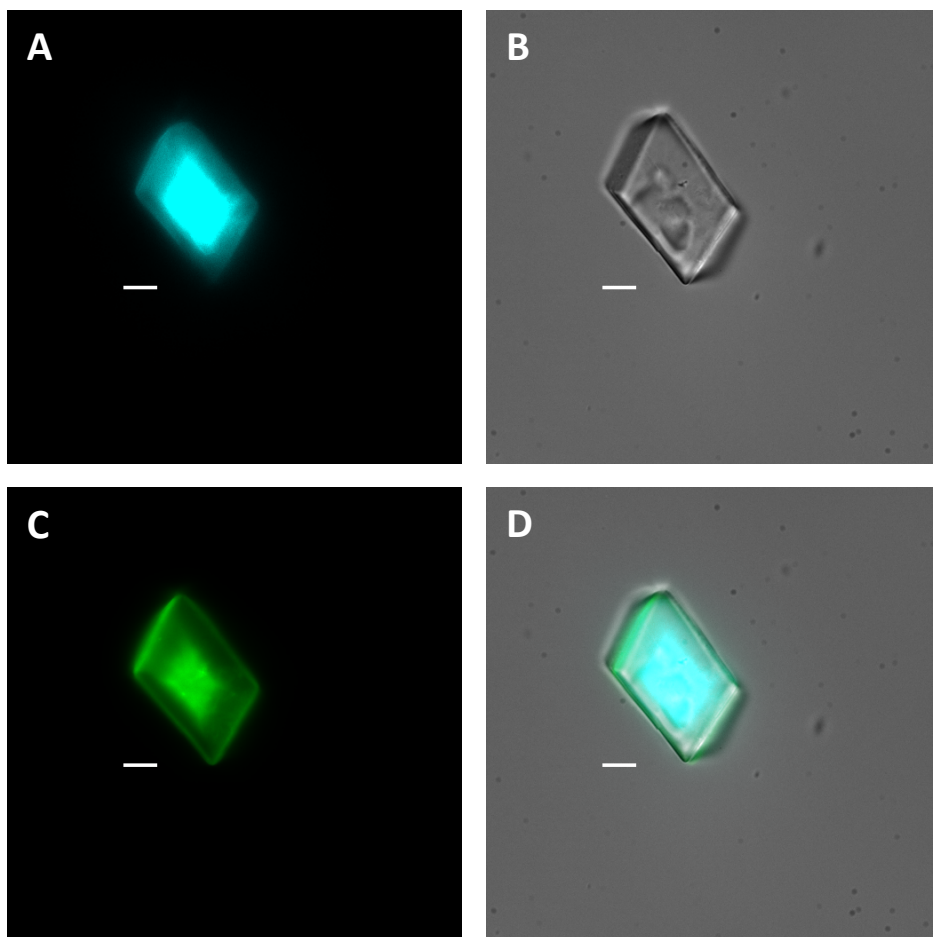


Figure S3: Optical microscopy images of a single crystal of FL@CD-MOF-161 upon excitation with light selected by a 482 nm band pass 35 nm filter. (A) Yb^{III}-centred emission in the NIR (λ_{em} : 996 nm band pass 70 nm, exposure time: 100 ms). (B) Brightfield. (C) Fluorescein-centred emission (λ_{em} : 550 nm band pass 88 nm, exposure time: 30 ms). (D) Merged. Objective 60x. Scale bar is 10 μ m.

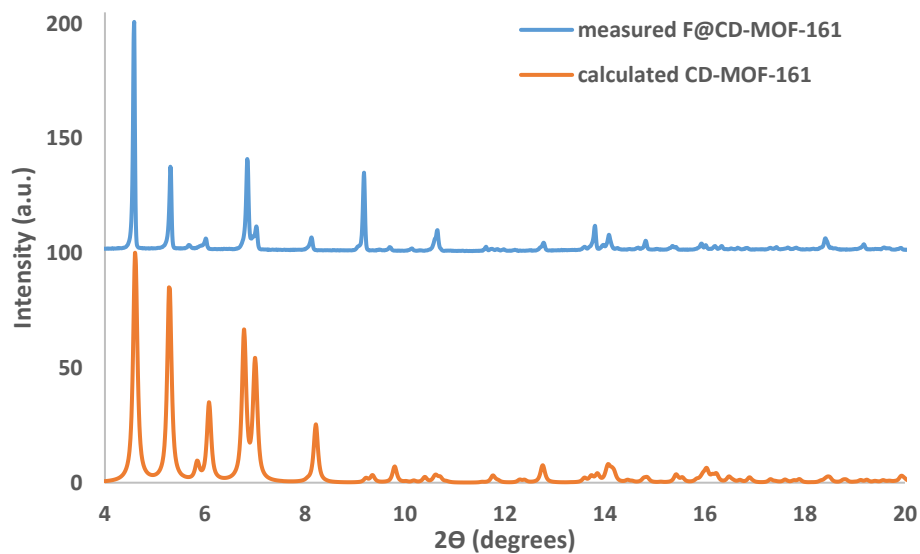


Figure S4: Experimental powder diffraction patterns recorded from FL@CD-MOF-161 (blue line) and calculated one determined from a CD-MOF-161 structure containing any fluorescein (orange line). The calculated pattern was obtained with Mercury software using the single-crystal structure recorded at 180 K.

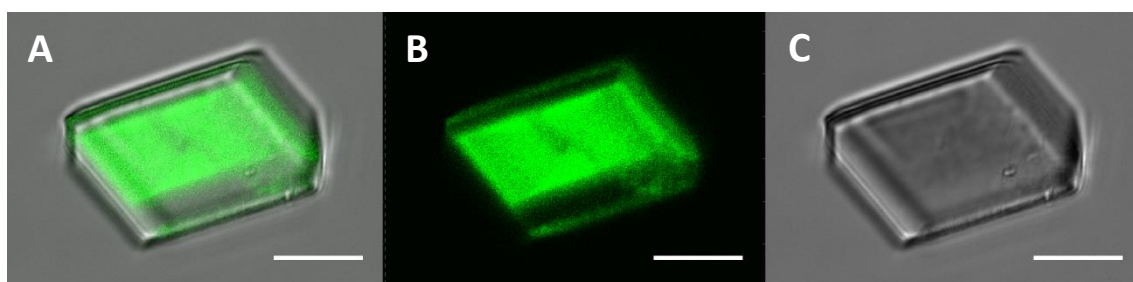


Figure S5: Confocal laser scanning microscopy images of a single crystal of FL@CD-MOF-161 (B) Fluorescein-centred emission (λ_{ex} : 488 nm, λ_{em} : 500 – 540 nm). The individual optical section of 0.370 μm thickness was imaged in a median position of the crystal along the z-axis. (C) Brightfield. (A) Merged. Objective 60x. Scale bar is 10 μm .

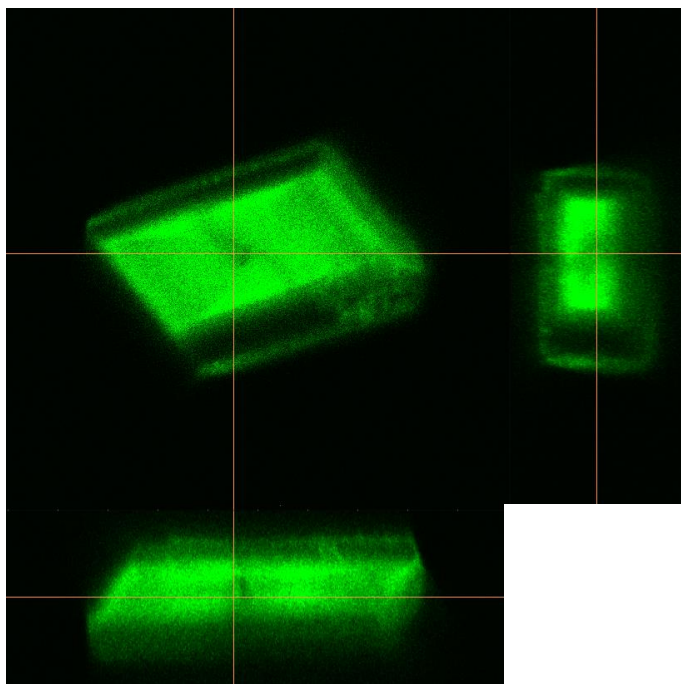


Figure S6: Confocal laser scanning microscopy images of a single crystal of FL@CD-MOF-161. Fluorescein-centred emission (λ_{ex} : 488 nm, λ_{em} : 500 – 540 nm). A series of optical sections of 0.370 μm thickness along the z-axis allowed to build the presented 3-axis projection. Objective 60x.

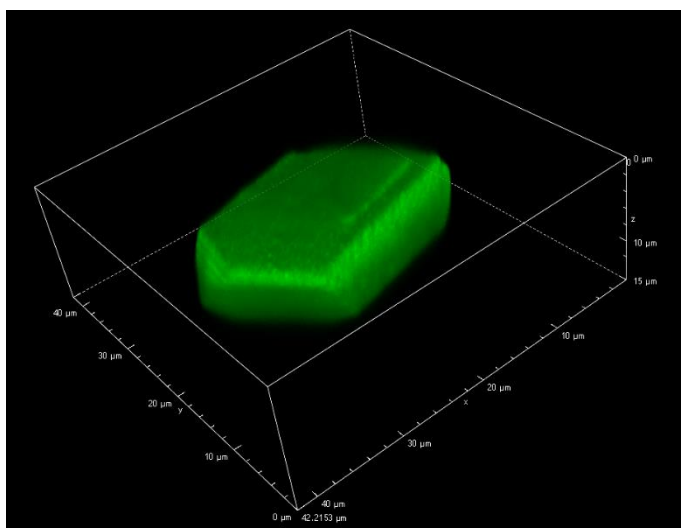


Figure S7: Confocal laser scanning microscopy image of a single crystal of FL@CD-MOF-161. Fluorescein-centred emission (λ_{ex} : 488 nm, λ_{em} : 500 – 540 nm). A series of optical sections of 0.370 μm thickness along the z-axis allowed to build the presented volume rendering. Objective 60x.

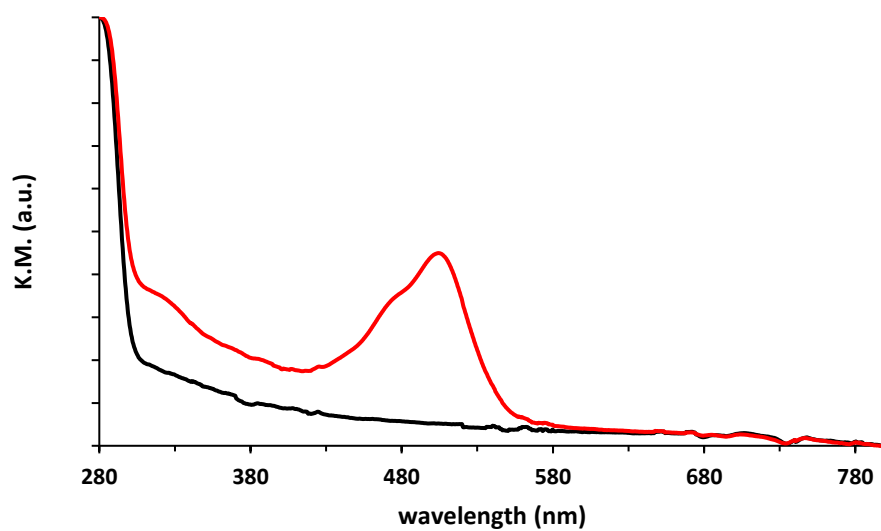


Figure S8. Normalized UV-vis diffuse reflectance spectra represented as Kubelka-Munk function of FL@CD-MOF-161 crystals (red line) and empty CD-MOF-161 (black line). All measurements were performed at room temperature.

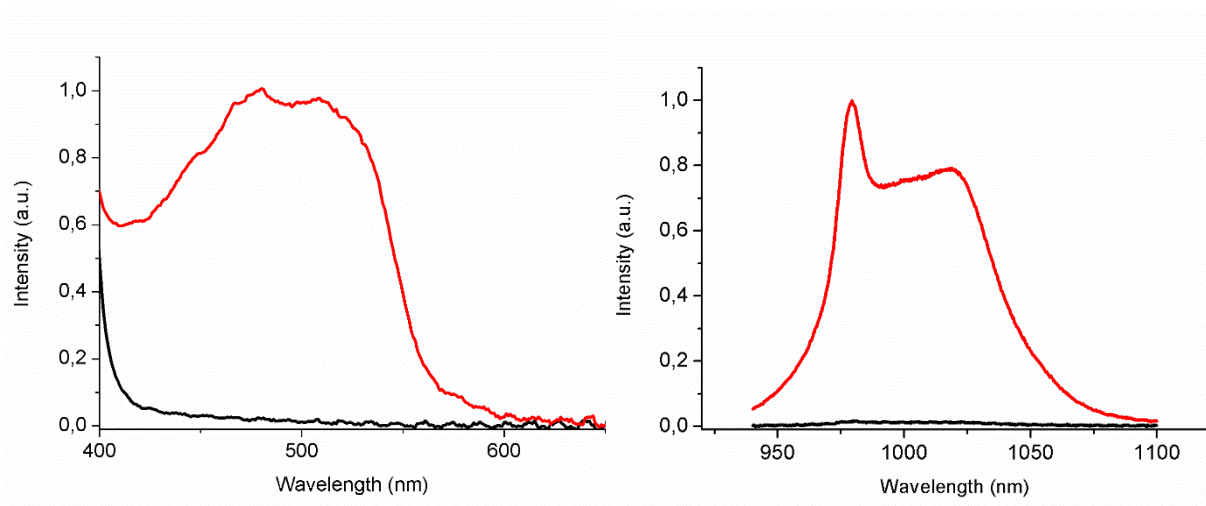


Figure S9: Corrected and normalized (left) excitation and (right) emission spectra of FL@CD-MOF-161 crystals (red line) and empty CD-MOF-161 crystals used as a control (black line) suspended in DMA at room temperature. Excitation spectra were recorded by monitoring the Yb³⁺ emission at 980 nm. Emission spectra were collected upon a 480 nm excitation.

Table S1. Luminescence lifetimes (τ_{obs}) and Yb³⁺-centred absolute quantum yields (Q_{Yb}^L) of freshly prepared and stored for 1 year FL@CD-MOF-161 crystals under DMA. ^[a] All measurements were performed at room temperature

| Sample | τ_{obs} (μs) ^[b] | Q_{Yb}^L (%) ^[c] |
|--------------|---|--------------------------------------|
| Fresh | $\tau_1 = 11.6(2)$, $B_1 = 65(2)$ %; $\tau_2 = 2.2(2)$, $B_2 = 25(3)$ %; $\tau_3 = 0.7(1)$, $B_3 = 10(3)$ % $\langle \tau \rangle = 10.8$ | 0.308(3) |
| After 1 year | $\tau_1 = 15.6(3)$, $B_1 = 74(7)$ %; $\tau_2 = 4.1(2)$, $B_2 = 18(4)$ %; $\tau_3 = 0.89(3)$, $B_3 = 8(4)$ % $\langle \tau \rangle = 14.9$ | 0.183(4) |

^[a] 2σ values are given between parentheses. ^[b] Under excitation at $\lambda_{\text{ex}} = 355$ nm; an average luminescence lifetime calculated using the formula: $\langle \tau \rangle = \frac{\sum_i B_i \tau_i^2}{\sum_i B_i \tau_i}$. ^[c] $\lambda_{\text{ex}} = 480$ nm.

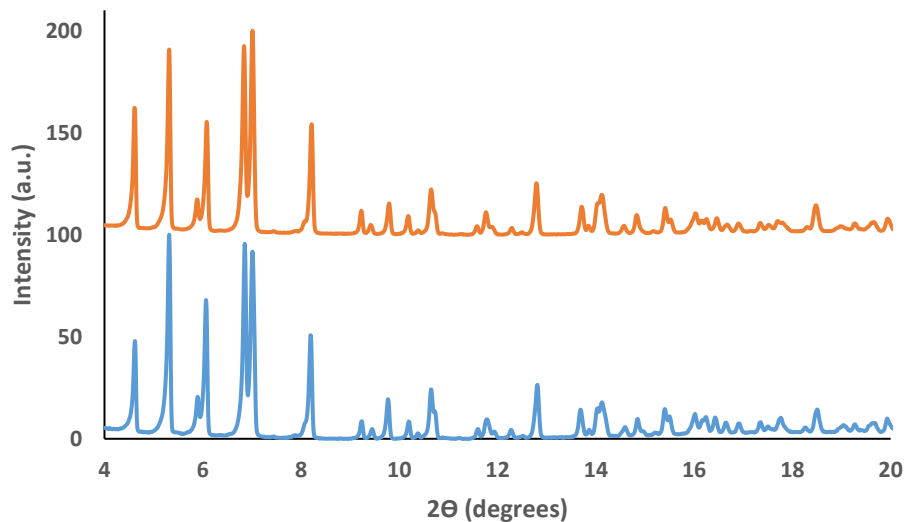


Figure S10: Powder diffraction patterns measured on freshly synthesized FL@CD-MOF-161 (orange line) and on one-year-old FL@CD-MOF-161 (blue line).

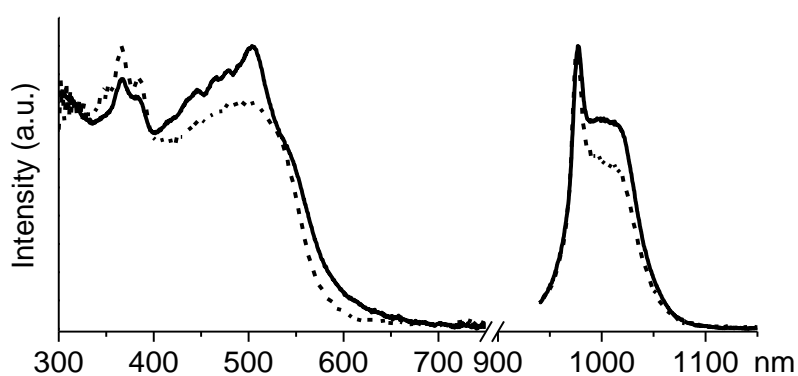


Figure S11. Corrected and normalized (left) excitation and (right) emission spectra of freshly prepared (solid traces) and stored during 1 year (dashed traces) FL@CD-MOF-161 crystals. Excitation spectra were recorded by monitoring the Yb^{3+} emission at 980 nm. Emission spectra were collected upon a 480 nm excitation. All measurements were performed at room temperature.

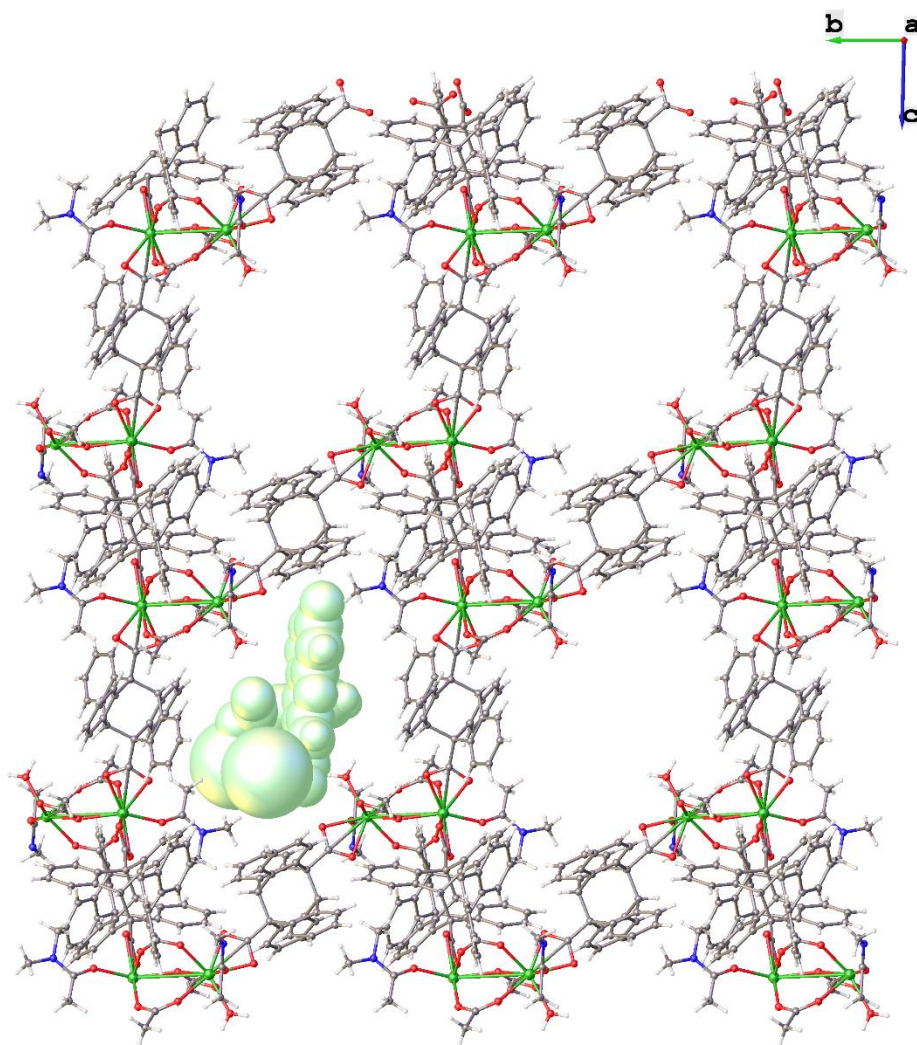


Figure S12: Crystal structure of a fluorescein disodium molecule fitted inside of a pore of the FL@CD-MOF-161.

Ytterbium metal ions are depicted in green, carbon in grey, oxygen in red, nitrogen in blue, hydrogen in white.

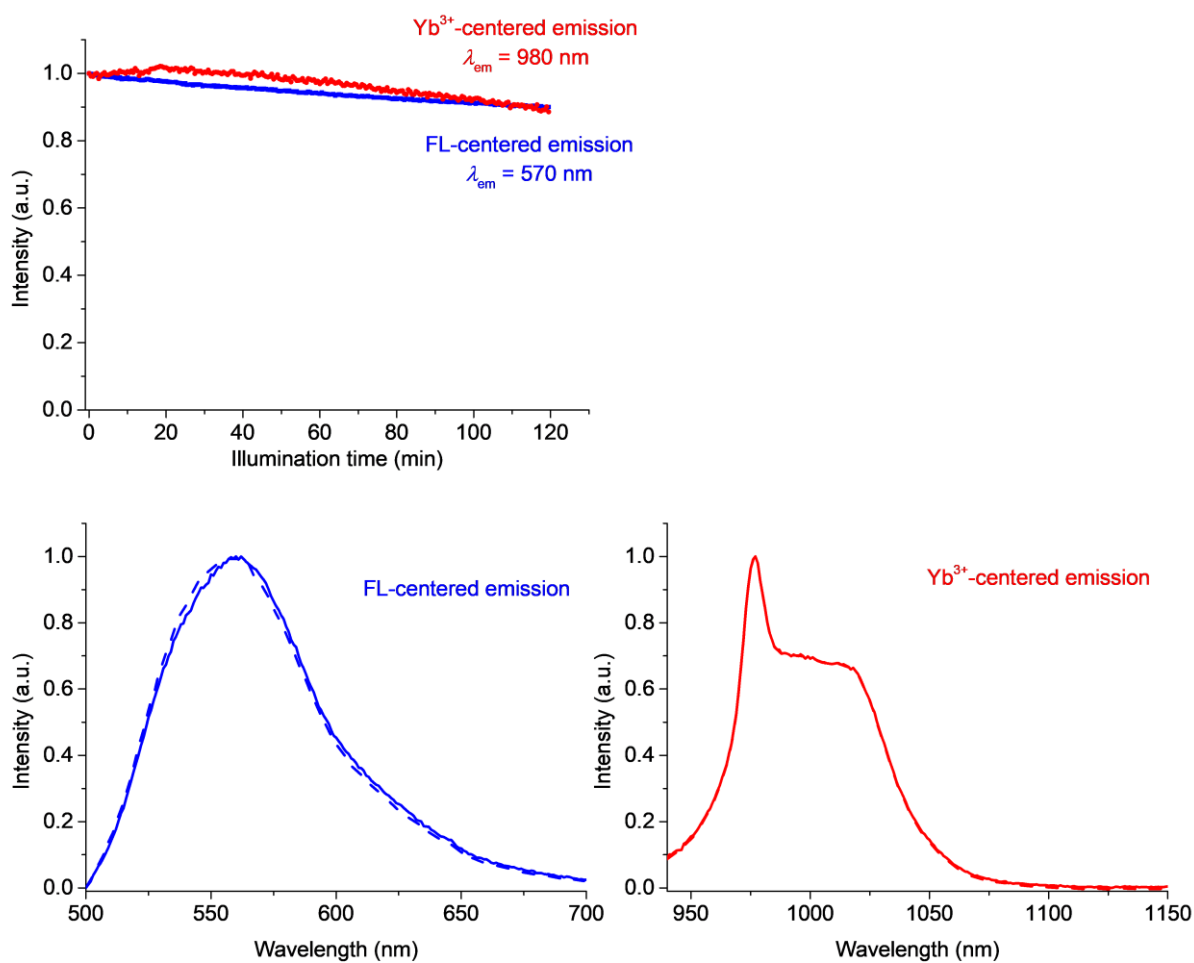


Figure S13. Photobleaching experiment performed on FL@CD-MOF-161 crystals upon continuous illumination at 480 nm (0.8 mW/mm^2) during 2 hours. (top) Changes in intensity of Yb³⁺-centred emission at 980 nm in red. Changes in intensity of FL-centred emission at 570 nm in blue. (bottom) Comparison of corrected and normalized emission spectra of FL@CD-MOF-161 crystals before (solid trace) and after (dashed trace) this photobleaching experiment ($\lambda_{\text{ex}} = 480 \text{ nm}$). FL-centered emission in blue. Yb³⁺-centered emission in red. All measurements were performed at room temperature.

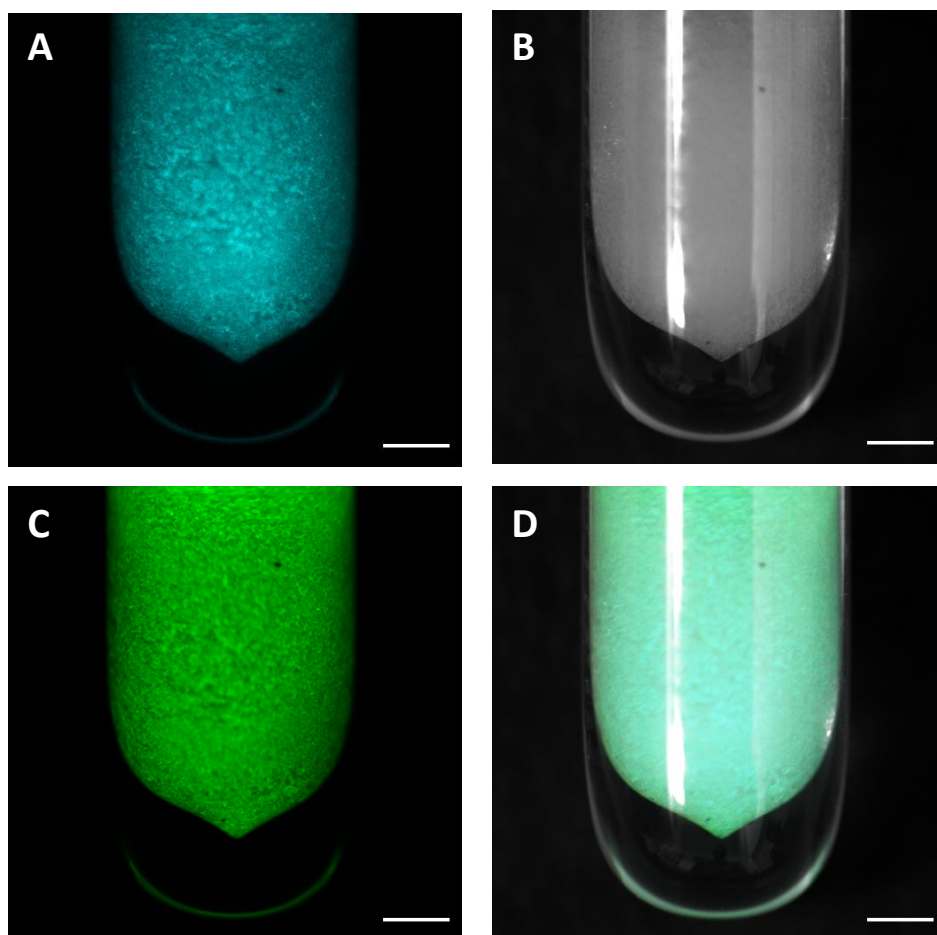


Figure S14: Optical macroscopy images of a quartz capillary filled with FL@CD-MOF-161 crystals upon excitation with light selected by a 482 nm band pass 35 nm filter. (A) Yb^{III}-centered emission in the NIR (λ_{em} : 996 nm band pass 70 nm, exposure time: 5 s). (B) Brightfield. (C) Fluorescein-centred emission (λ_{em} : 550 nm band pass 88 nm, exposure time: 20 ms). (D) Merged. Macro-objective 2x. Scale bar is 500 μm .

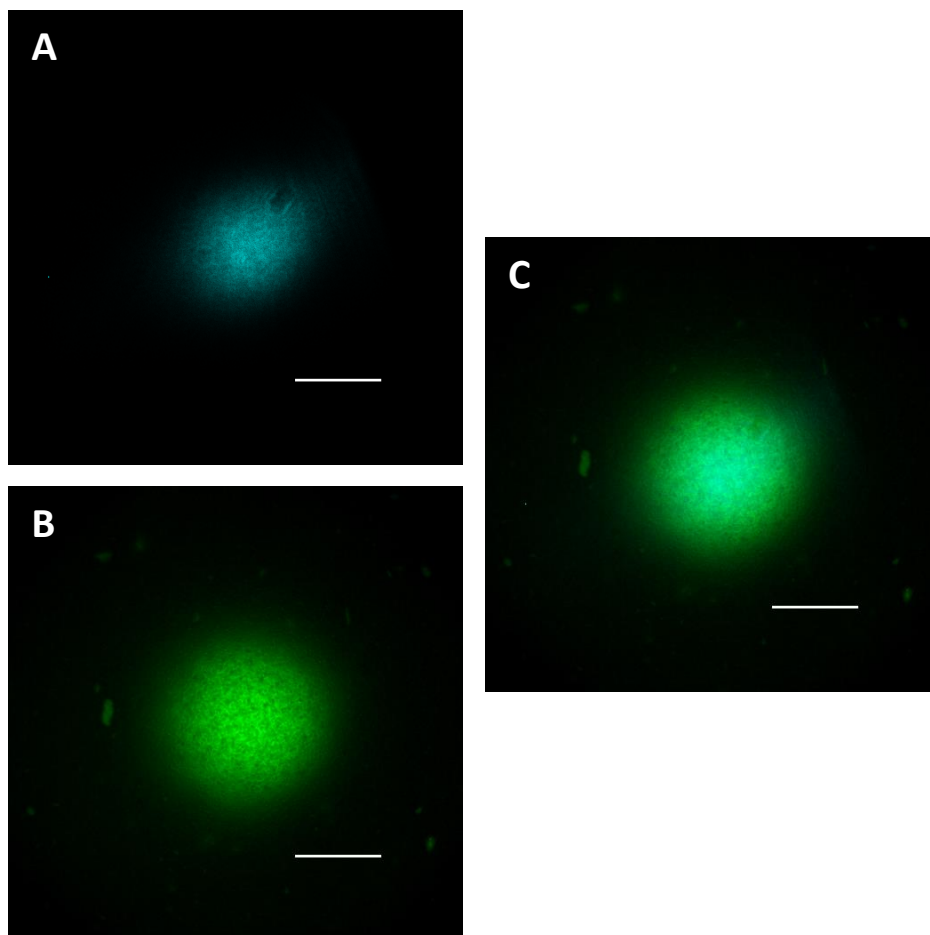


Figure S15: Optical macroscopy pictures of a quartz capillary filled with FL@CD-MOF-161 crystals covered by a black mask with a hole of 500 μm in diameter. This assembly is located below a 1 mm thick bio-mimicking phantom tissue and is excited with light selected by a 482 nm band pass 35 nm filter. (A) Yb^{III}-centred emission in the NIR (λ_{em} : 996 nm band pass 70 nm, exposure time: 30 s). (B) Fluorescein-centred emission (λ_{em} : 550 nm band pass 88 nm, exposure time: 100 ms). (C) Merged. Macro-objective 5x. Scale bar is 500 μm .